JOURNAL OF BACTERIOLOGY, Feb. 1992, p. 711–724
0021-9193/92/030711-14$02.00/0
Copyright © 1992, American Society for Microbiology
Vol. 174, No. 3

Nucleotide Sequence and Functional Analysis of the Complete Phenol/3,4-Dimethylphenol Catabolic Pathway of *Pseudomonas* sp. Strain CF600

VICTORIA SHINGLER,[1]* JUSTIN POWLOWSKI,[2] AND ULRICA MARKLUND[1]

The Unit for Applied Cell and Molecular Biology, The University of Umeå, S-901 87 Umeå, Sweden,[1] and Department of Chemistry and Biochemistry, Concordia University, Montreal, Quebec H3G IM8, Canada[2]

Received 12 August 1991/Accepted 11 November 1991

The *meta*-cleavage pathway for catechol is one of the major routes for the microbial degradation of aromatic compounds. *Pseudomonas* sp. strain CF600 grows efficiently on phenol, cresols, and 3,4-dimethylphenol via a plasmid-encoded multicomponent phenol hydroxylase and a subsequent *meta*-cleavage pathway. The genes for the entire pathway were previously found to be clustered, and the nucleotide sequences of *dmpKLMNOPBC* and *D*, which encode the first four biochemical steps of the pathway, were determined. By using a combination of deletion mapping, nucleotide sequence determinations, and polypeptide analysis, we identified the remaining six genes of the pathway. The fifteen genes, encoded in the order *dmpKLMNOPQBCDEFGHI*, lie in a single operon structure with intergenic spacing that varies between 0 to 70 nucleotides. Homologies found between the newly determined gene sequences and known genes are reported. Enzyme activity assays of deletion derivatives of the operon expressed in *Escherichia coli* were used to correlate *dmpE*, *G*, *H*, and *I* with known *meta*-cleavage enzymes. Although the function of the *dmpQ* gene product remains unknown, *dmpF* was found to encode acetaldehyde dehydrogenase (acylating) activity (acetaldehyde:NAD$^+$ oxidoreductase [coenzyme A acylating]; E.C.1.2.1.10). The role of this previously unknown *meta*-cleavage pathway enzyme is discussed.

The central role of catecholic intermediates in aerobic microbial degradation of aromatic compounds is well established. Catechol (1,2-dihydroxybenzene) itself is an intermediate in the degradation of compounds such as benzoate, naphthalene, salicylate, and phenol, and substituted catechols are intermediates in the catabolism of methylated and chlorinated derivatives of these compounds (13, 34). A diverse array of enzymes can be elaborated to convert aromatic compounds to central catecholic intermediates. However, the reactions used for oxygenative ring fission of the catechol and the subsequent conversion to Krebs cycle intermediates are limited to one of two metabolic alternatives: those of the *ortho*- and *meta*-cleavage pathways. The *ortho*-cleavage pathways involve ring cleavage between the two hydroxyl groups followed by a well-defined series of reactions leading to β-ketoadipate (reviewed in reference 13). The alternative *meta*-cleavage pathway involves ring cleavage adjacent to the two catechol hydroxyls, followed by degradation of the ring cleavage product to pyruvate and a short-chain aldehyde (Fig. 1). The use of one pathway or the other is dependent upon the microbial species and/or the nature of the growth substrate.

The *meta*-cleavage pathway was first studied in *Pseudomonas* strains that can grow at the expense of phenol and cresols (14, 29). Since then, the role of the *meta*-cleavage pathway in aromatic biodegradation by bacteria of many genera, including species of *Azotobacter* and *Alcaligenes* and numerous species of *Pseudomonas*, has been demonstrated (2, 13, 23, 36). In addition, reactions of the lower part of the pathway are involved in the degradation of phenylpropionates by *Escherichia coli* (8). From this variety of sources, a wealth of information has accumulated regarding pathway chemistry, gene organization and regulation, and, to a lesser extent, gene structure and enzymology.

The most comprehensively studied *meta*-cleavage pathway is that of the IncP-9 TOL plasmid pWWO, which encodes a toluene degradation pathway of *Pseudomonas putida*. The *meta*-cleavage pathway genes are located in an operon that encodes the enzymes for conversion of benzoate, via catechol, to central metabolites; a separate operon encodes the enzymes required to convert toluene and xylenes to the corresponding benzoates. The TOL *meta*-cleavage operon comprises 13 structural genes, of which 2, *xylT* and *xylQ*, have no known function (19). The remaining genes encode the enzymes required for the conversion of benzoate to catechol and then to pyruvate and acetaldehyde via the reactions shown in Fig. 1. The enzymes of the pathway from the ring fission enzyme downward have been studied to various extents. Whereas catechol 2,3-dioxygenase, for example, has been the subject of many studies, other enzymes, such as 4-hydroxy-2-oxovalerate aldolase and 2-hydroxymuconic semialdehyde dehydrogenase, have apparently not even been purified. Many features of the TOL *meta*-cleavage pathway gene organization and enzyme function are preserved in other aromatic catabolic pathways in *Pseudomonas* species (for a review, see reference 2).

The *meta*-cleavage pathway also functions in the degradation of phenols and methyl-substituted phenols by a number of different *Pseudomonas* species (14, 26, 37, 40). *Pseudomonas* sp. strain CF600 can grow efficiently with phenol, cresols, or 3,4-dimethylphenol (3,4-dmp) as the sole carbon and energy source (40). The catabolic pathway for these substrates is encoded on pVI150, an IncP-2 megaplasmid, and involves hydroxylation followed by a *meta*-cleavage pathway. The genes for the enzymes of this pathway were previously found to be clustered, and the nucleotide sequences of the genes involved in the first four biochemical

* Corresponding author.

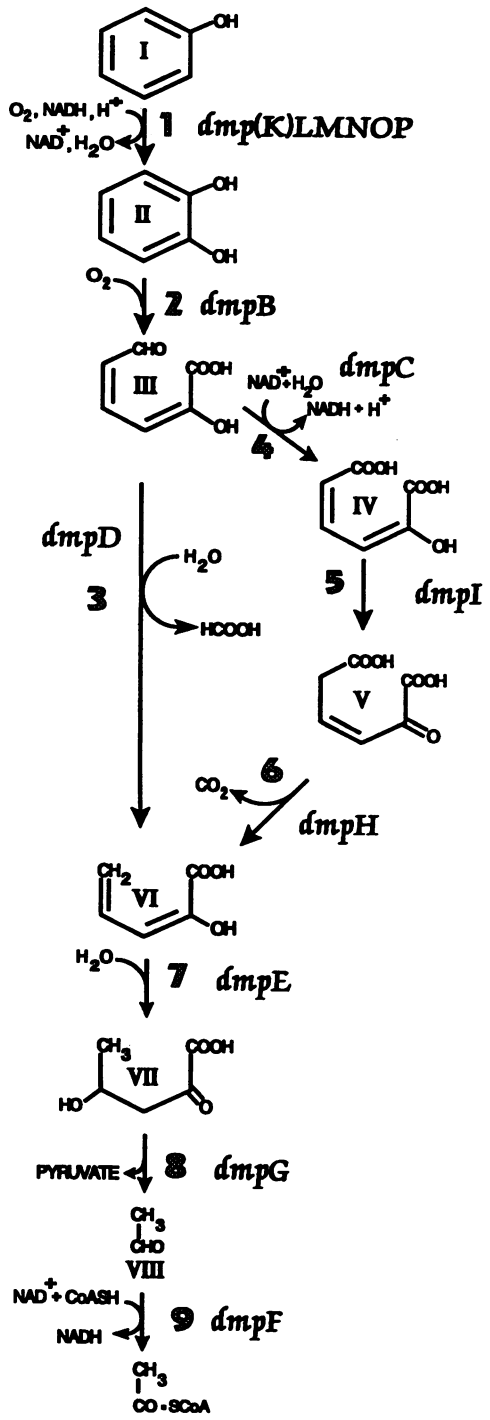

FIG. 1. The pVI150 plasmid-encoded catabolic pathway for the dissimilation of phenol and its methylated derivatives. Enzyme structural genes are defined in the text. Compounds: I, phenol; II, catechol; III, 2-hydroxymuconic semialdehyde; IV, 4-oxalocrotonate, enol form (2-hydroxyhexa-2,4-diene-1,6-dioate); V, 4-oxalocrotonate, keto form (2-oxohex-3-ene-1,6-dioate); VI, 2-oxopent-4-enoate; VII, 4-hydroxy-2-oxovalerate; VIII, acetaldehyde. Enzymes: 1, phenol hydroxylase (PH); 2, catechol 2,3-dioxygenase (C23O); 3, 2-hydroxymuconic semialdehyde hydrolase (2HMSH); 4, 2-hydroxymuconic semialdehyde dehydrogenase (2HMSD); 5, 4-oxalocrotonate isomerase (4OI); 6, 4-oxalocrotonate decarboxylase (4OD); 7, 2-oxopent-4-enoate hydratase (OEH); 8, 4-hydroxy-2-oxovalerate aldolase (HOA); 9, acetaldehyde dehydrogenase (acylating) (ADA).

steps of the pathway, *dmpK*, *L*, *M*, *N*, *O*, *P*, *B*, *C*, and *D*, have been determined (3, 4, 30, 31).

The *dmpKLMNOP* genes are involved in the conversion of phenol to catechol. Only the polypeptide products of the *dmpLMNOP* genes, namely, P1, P2, P3, P4, and P5, are required for in vitro activity of a multicomponent phenol hydroxylase (33). The function of P0, the product of *dmpK*, is unknown. Although P0 is not required for in vitro phenol hydroxylase activity, it is required in vivo, together with P1 through P5, for growth on phenol by a pseudomonad that can catabolize catechol (30). The *dmpKLMNOP* genes are arrayed in an operon structure with no more than 70 bp between any two genes.

The *dmpB*, *C*, and *D* genes encode enzymes (Fig. 1) that have analogs in *meta*-cleavage pathways for catabolism of a variety of aromatic compounds. The gene order of *dmpB*, *C*, and *D* is identical to that of the analogous genes of the TOL pathway, and the polypeptide product sizes are similar (3). The ring-cleavage enzyme catechol 2,3-dioxygenase is encoded by *dmpB* (4) and catalyzes the conversion of catechol to 2-hydroxymuconic semialdehyde. The coding region for catechol 2,3-dioxygenase is located approximately 350 bp downstream from *dmpP*. The amino acid sequence of this enzyme was found to be 83 to 87% homologous to catechol 2,3-dioxygenase from the TOL and NAH7 naphthalene catabolic pathways (4). The *dmpC* and *dmpD* genes encode the first enzymes of the branches of the *meta*-cleavage pathway: 2-hydroxymuconic semialdehyde dehydrogenase and 2-hydroxymuconic semialdehyde hydrolase, respectively. The *dmpB*, *C*, and *D* genes are closely linked with intergenic spacing of 38 and 11 bp (31). Although nucleotide sequence information for isofunctional genes is not available, the product of *dmpC*, 2-hydroxymuconic semialdehyde dehydrogenase, exhibits approximately 40% sequence identity with aldehyde dehydrogenases from eukaryotic sources (31).

Here we report gene locations, nucleotide sequences, polypeptide analysis, and associated activities for the rest of the *meta*-cleavage pathway genes of *Pseudomonas* sp. strain CF600. This work completes the gene structure information for the *meta*-cleavage enzymes and provides evidence that the phenol/3,4-dmp catabolic operon is composed of 15 genes. Moreover, the nucleotide sequence information includes the discovery of a new operon-encoded *meta*-cleavage pathway enzyme that can metabolize acetaldehyde. This work should considerably aid future efforts to increase the comparatively meager knowledge of *meta*-cleavage pathway enzymology.

MATERIALS AND METHODS

Bacterial strains and plasmids. The bacterial strains and plasmids used in this study are listed in Table 1. Plasmids were introduced into *E. coli* strains by the procedure of Kushner (27) and into *Pseudomonas* sp. strain PB2701 either by conjugation from *E. coli* S17-1 or by electroporation with a Bio-Rad Gene Pulser. Ampicillin (100 μg/ml) and carbenicillin (1 to 2 mg/ml) were used for selection of plasmid-encoded β-lactamase in *E. coli* and *Pseudomonas* strains, respectively.

Plasmids were constructed by using standard recombinant techniques. The plasmids designated pVI are based on the broad-host-range *tac* expression vectors pMMB66HE and pMMB66EH or derivatives thereof (pMMB66HEΔ and pMMB66EHΔ, respectively). Plasmids that are based on the pMMB66Δ vectors are indicated by a Δ symbol. The extent

TABLE 1. Bacterial strains and plasmids

Strain or plasmid	Relevant properties[a]	Reference or source
E. coli		
S17-1	r^- m^+ Tp^r Sm^r Mob^+	41
DH5	r^- m^+ *recA1*	17
CSR603	Maxicell strain	38
Pseudomonas strains		
Pseudomonas sp. strain CF600	Phenol/3,4-dmp degrader	40
P. putida U	Phenol degrader (ATCC 17514)	14
P. putida PB2701	r^- m^+ Sm^r derivative of KT2440	MBSC[b]
Plasmids		
pBluescript SK(+)	Ap^r cloning and sequencing vector	Stratagene
pMMB66HE and EH	Ap^r, RSF1010 based *tac* promoter expression vectors carrying $lacI^q$	16
pMMB66HEΔ and EHΔ	Derivatives of pMMB66HE and EH without the $lacI^q$ repressor gene	40
pVI264	*dmpKLMNOPQBCDE*, *Bgl*II-*Eco*RI fragment (kb 0.25–10.0) (Fig. 2)	3
pVI265	*dmpKLMNOPQBCDEFGHI*, *Bgl*II-*Bam*HI fragment (kb 0.25–19.9) (Fig. 2)	3
pVI298	*dmpKLMNOPQBCDEFGHI*, *Bgl*II-*Nru*I fragment (kb 0.25–15.0) (Fig. 2)	This study
pVI299	*dmpKLMNOPQBCDEFGHI*, *Bgl*II-*Pvu*II fragment (kb 0.25–13.5) (Fig. 2)	This study
pVI300Δ	*dmpQ*, *Bal* 31-*Pst*I fragment (bp 5367–6240) (Fig. 4)	This study
pVI301Δ	*dmpDE*, *Hpa*I-*Eco*RI fragment (bp 8047–10051) (Fig. 4)	This study
pVI302Δ	*dmpGHI*, *Eco*RI-*Bam*HI fragment (bp 10051–19900) (Fig. 4)	This study
pVI303Δ	*dmpDEFGH*, *Hpa*I-*Xho*I fragment (bp 8047–12784) (Fig. 4)	This study
pVI304Δ	*dmpGH*, *Eco*RI-*Xho*I fragment (bp 10051–12784) (Fig. 4)	This study
pVI305Δ	*dmpGHI*, *Eco*RI-*Bgl*II fragment (bp 10051–16450) (Fig. 4)	This study
pVI306Δ	*dmpFGHI*, *Nru*I-*Nru*I fragment (bp 9105–15000) (Fig. 4)	This study
pVI307Δ	*dmpFGHI*, *Nru*I-*Pvu*II fragment (bp 9105–13489) (Fig. 4)	This study
pVI308Δ	*dmpD*, *Hpa*I-*Sac*I fragment (bp 8047–9070) (Fig. 4)	This study
pVI309Δ	*dmpE*, *Dde*I-*Eco*RI fragment (bp 9033–10051) (Fig. 4)	This study
pVI310Δ	*dmpF*, *Sal*I-*Sal*I fragment (bp 9790–10929) (Fig. 4)	This study
pVI311Δ	*dmpF*, *Nru*I-*Not*I fragment (bp 9105–11702) (Fig. 4)	This study
pVI312Δ	*dmpG*, *Sau*I-*Bst*EII fragment (bp 10785–11921) (Fig. 4)	This study
pVI313Δ	*dmpH*, *Not*I-*Xho*I fragment (bp 11702–12784) (Fig. 4)	This study
pVI314Δ	*dmp*I, *Sca*I-*Pvu*II fragment (bp 12670–13489) (Fig. 4)	This study
pVI315Δ	*dmpEH*, *Dde*I-*Xho*I fragment (bp 9033–12784) (deleted between bp 10051–11702) (Fig. 4)	This study
pVI316Δ	*dmpFG*, *Nru*I-*Kpn*I fragment (bp 9105–12553) (Fig. 4)	This study

[a] r and m refer to host restriction and modification systems, respectively. Antibiotic resistance abbreviations: Ap^r, ampicillin; Sm^r, streptomycin; Tp^r, trimethoprim. The catabolic *dmp* genes are described in the text. Base pair coordinates are given relative to the last base of the restriction enzyme recognition sites.

[b] MBSC, M. Bagdasarian strain collection.

of *Pseudomonas* sp. strain CF600-derived DNA present in these plasmids is listed in Table 1 and illustrated in Fig. 2 and 4.

Culture conditions. Cells for crude extract preparation were grown as follows. *Pseudomonas* sp. strain CF600 was grown at 30°C in minimal medium, supplemented with 2.5 mM carbon source and trace metals (33), for approximately 15 h after inoculation (1:200) of Luria broth-grown cells. Additional carbon source was added at 2- to 3-h intervals, and growth was continued for approximately 6 h. *E. coli* cells were grown at 37°C in Luria broth for 12 to 15 h after inoculation (1:1,000). Induction of the $lacI^q$-regulated *tac* promoter of pMMB66HE- and pMMB66EH-based plasmids was achieved by the addition of isopropyl-β-D-thiogalactopyranoside (IPTG), to a final concentration of 0.5 mM, at 3 h postinoculation.

Analysis of plasmid-encoded polypeptides. Plasmids were introduced into the maxicell CSR603 strain; plasmid-encoded polypeptides were prepared, labeled with L-[^{35}S]methionine (Amersham), and analyzed essentially as described previously (38). To aid in the separation of small polypeptides, sodium dodecyl sulfate-polyacrylamide gel electrophoresis (SDS-PAGE) was performed with the addition of 32 mM NaCl in the analytical gel (28, 30). Size estimations of polypeptides were performed by using an LMW calibration kit (no. 17-044601) and peptide molecular mass standards (no. 17-055101) from Pharmacia.

Nucleotide sequence determinations. Nucleotide sequences were determined directly from plasmids by using a Pharmacia DNA sequencing kit (no. 27-168201). To determine the nucleotide sequences of the previously unsequenced regions of the operon, subfragments were cloned into the polycloning site of a pBluescript SK(+) sequencing vector (Stratagene). Ordered deletion libraries of the resulting plasmids were generated by using exonuclease III and mung bean nuclease essentially as described in the Stratagene Exo/Mung DNA sequencing manual. Both strands were sequenced and the junctions of fragments were confirmed by using custom-designed oligonucleotides.

Chemicals. All chemicals used for the preparation of buffers were reagent grade or better. All coenzymes were obtained from either Sigma Chemical Co. or Boehringer Mannheim. Solutions of 2-oxopent-4-enoic acid were synthesized from L-allylglycine essentially as described by Collinsworth et al. (12). 4-Hydroxy-2-oxovalerate was prepared by mild alkaline hydrolysis of 4-methyl-2-oxobutyrolactone (14). 4-Oxalocrotonate was a gift from Peter Williams (University of Wales, Bangor). Equilibrium mix-

tures of the keto and enol forms of this compound were prepared by mixing an ethanolic solution of 4-oxalocrotonate with 50 mM Tris-HCl (pH 7.4) and allowing the solution to stand at room temperature for 1 h before use (20).

L-(*S*)-4-Methyl-2-oxobutyrolactone was synthesized essentially as described by Burlingame and Chapman (8, 9) by using treated crude extracts of phenol-grown *P. putida* U (9, 14) or *Pseudomonas* sp. strain CF600 to accumulate the lactone from catechol. Rather than using continuous extraction with diethyl ether, we used acidified reaction mixtures saturated with sodium chloride and then extracted four times with equal volumes of ethyl acetate. Yields from the different reaction mixtures were approximately 50% of the theoretical yield. The compound synthesized from *P. putida* U was previously characterized as the L-(*S*) isomer (9). The compounds obtained with *P. putida* U or *Pseudomonas* sp. strain CF600 extracts were indistinguishible on the basis of melting point (70 to 73°C) or circular dichroism measurements. This establishes the stereochemistry of 4-hydroxy-2-oxovalerate formed in *Pseudomonas* sp. strain CF600 as L-(*S*).

Crude extract preparation. Cells used for making crude extracts were harvested, washed twice with cold 10 mM Na^+-K^+ phosphate buffer (pH 7.5), and then used immediately or stored at −70°C as a frozen paste. In preparation for sonication, cells were resuspended in either 50 mM Na^+-K^+ phosphate buffer (pH 7.5) or 50 mM Tris-HCl (pH 7.4) buffer containing 2 mM dithiothreitol. Crude extracts were prepared by sonication of cell suspensions and then centrifugation at 83,000 × *g* for 1 h. The supernatants were kept on ice and used within 30 h of preparation.

Estimation of protein concentration. The protein concentrations in cell extracts were estimated by using a BCA (bicinchoninic acid) assay (Pierce Chemical Co.) with bovine serum albumin as the standard. The protocol for 60°C described in the manufacturer's instructions was used, with a modification (7) to eliminate interference from the dithiothreitol in the crude extracts.

Enzyme activity assays. All enzyme assays were performed at 25°C except for the acetaldehyde dehydrogenase (acylating) assay, which was carried out at 20°C.

4-Oxalocrotonate isomerase was assayed by measuring the decrease in A_{295}. The reaction conditions were essentially as described previously (36), except that the assay was conducted in 10 mM Na^+-K^+ phosphate buffer (pH 7.4) (0.5 ml). One unit of enzyme activity is defined as the amount of enzyme required to cause an A_{295} decrease of 1.0 per min in a 3-ml reaction volume (36).

4-Oxalocrotonate decarboxylase activity was measured by determining the amount of substrate remaining, from the A_{350} after the reaction mixtures were quenched with NaOH-EDTA (18), at 15-s intervals over a 1-min period. The reaction mixtures (0.5 ml) contained 50 mM Tris-HCl (pH 7.4), 2.7 mM $MgSO_4$, and 125 μM 4-oxalocrotonate (equilibrium keto-enol mixture). To ensure that the formation of the keto form of 4-oxalocrotonate was not rate limiting in the later part of the reaction, 5.5 U of 4-oxalocrotonate isomerase, obtained by heat treatment (20, 36) of extracts from cells harboring pVI314Δ, was added to the assays with extracts that lacked this activity. One unit of activity is defined as the amount of enzyme required to catalyze the conversion of 1 μmol of substrate per min.

2-Oxopent-4-enoate hydratase activity was determined by the method of Collinsworth et al. (12), except that the buffer used was 45 mM Tris-HCl (pH 7.2), and 2.9 mM $MgSO_4$ was used in place of $MnCl_2$ (20). As defined by Collinsworth et al. (12), 1 U of activity is the amount of enzyme required to cause a decrease in A_{265} 1.0 per min in a 3-ml reaction volume.

The assay for 4-hydroxy-2-oxovalerate aldolase was carried out by monitoring the oxidation of NADH (A_{340}) in the presence of excess lactate dehydrogenase, which reduces pyruvate formed by the action of the aldolase (36). Reaction mixtures (1 ml) contained 46 mM *N*-2-hydroxyethylpiperazine-*N'*-2-ethanesulfonic acid buffer (pH 8.0), 1 mM $MnCl_2$, 260 μM NADH, 260 μM 4-hydroxy-2-oxovalerate, 28 *U* of lactate dehydrogenase, and 0.4 to 0.5 mg of crude extract protein. The reaction was initiated by the addition of 4-hydroxy-2-oxovalerate, and rates were corrected for the presence of NADH oxidase activity. *Pseudomonas* extracts contained high levels of alcohol dehydrogenase activity, so that, in the absence of lactate dehydrogenase, acetaldehyde formed by the aldolase could then be reduced by this enzyme. Thus, in phenol-grown *Pseudomonas* extracts in the absence of lactate dehydrogenase, NADH was consumed at approximately 50% of the rate observed in the presence of lactate dehydrogenase. In contrast, the alcohol dehydrogenase activity in *E. coli* extracts was very low, so that, in the absence of lactate dehydrogenase, extracts that exhibited aldolase activity did so at a rate of only 15 to 20% of that observed in the presence of lactate dehydrogenase. One unit of activity is defined as the amount of enzyme required to catalyze the oxidation of 1 μmol of NADH per min in the presence of excess lactate dehydrogenase.

The standard assay adopted for measurement of acetaldehyde dehydrogenase (acylating) activity involved monitoring the coenzyme A-stimulated reduction of NAD^+ (A_{340}). Assay mixtures (1 ml) contained 50 mM Na^+-K^+ phosphate buffer buffer (pH 7.5), 285 μM NAD^+, 10 mM acetaldehyde, and 0.2 to 0.4 mg of crude extract protein. The A_{340} of this mixture was monitored for 1 min, and the reaction was then initiated by the addition of coenzyme A (100 μM). One unit of activity is defined as the amount of enzyme required to reduce 1 μmol of NAD^+ per min in the presence of coenzyme A under these conditions.

Nucleotide sequence accession numbers. The nucleotide sequence data in this paper have been submitted to the EMBL data library under accession numbers X60835 and X60836.

RESULTS

Mapping of the phenol/3,4-dmp operon. The plasmid-encoded phenol/3,4-dmp catabolic pathway of *Pseudomonas* sp. strain CF600 involves a multicomponent phenol hydroxylase and a subsequent *meta*-cleavage pathway (Fig. 1). The genes for the enzymes of this pathway was previously found to be clustered on an approximately 20-kb *Sac*I-to-*Bam*HI fragment (3). The nucleotide sequence of the genes involved in the first four biochemical steps of the pathway, *dmpK*, *L*, *M*, *N*, *O*, *P*, *B*, *C*, and *D*, was previously determined, allowing unambiguous location within the 20-kb *Sac*I-to-*Bam*HI fragment (Fig. 2).

Expression of the 20-kb *Sac*I-to-*Bam*HI fragment confers on pseudomonads the ability to grow on phenol and its methylated derivatives *m*-, *o*-, and *p*-cresol and 3,4-dmp. The location of *dmpK*, *L*, *M*, *N*, *O*, *P*, *B*, *C*, and *D* within this fragment suggests that the remaining genes of the pathway are encoded downstream of *dmpD*. To further define the location of the pathway genes, deletion derivatives of pVI265, which expresses most of the 20-kb *Sac*I-to-*Bam*HI fragment, were constructed and tested for their

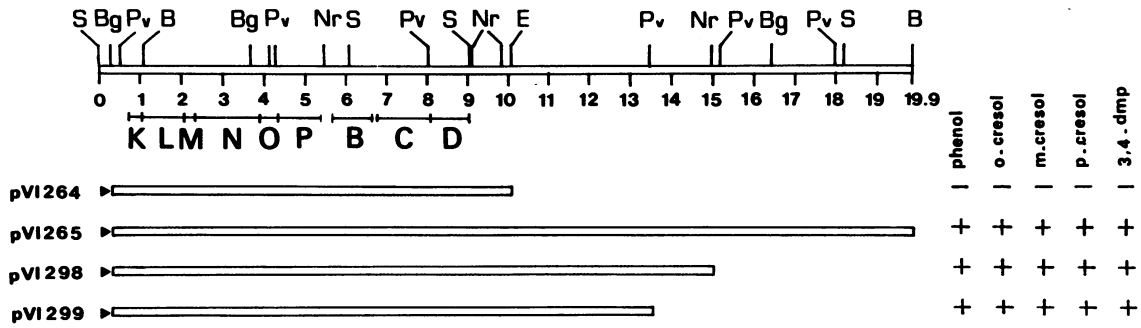

FIG. 2. Restriction map of cloned pVI150 DNA. Arrowheads indicate the direction of transcription from the *tac* promoter of the expression vector. The location of previously sequenced phenol catabolic genes are shown. Coordinates of restriction endonuclease recognition sites are given in kilobases. B, *Bam*HI; Bg, *Bgl*II; E, *Eco*RI; Nr, *Nru*I; Pv, *Pvu*II; S, *Sac*I. The ability of *P. putida* PB2701 harboring the plasmids to grow on M9 salts (3) supplemented with different carbon sources and IPTG (0.5 mM) is indicated.

ability to confer growth on phenol and methylphenols. The results of these experiments (Fig. 2) demonstrate that a 13.25-kb *Bgl*II-to-*Pvu*II fragment is sufficient to encode the entire phenol/3,4-dmp catabolic pathway.

Nucleotide sequence of the phenol/3,4-dmp genes. The complete nucleotide sequence of the 13.25-kb *Bgl*II-to-*Pvu*II fragment was determined as described in Materials and Methods. The sense strands of the previously unsequenced regions are shown in Fig. 3, along with translation of six open reading frames (ORFs) that are preceded by putative ribosome binding sites. The location, size, intergenic spacing, and G+C contents of these ORFs relative to those of known genes of the pathway are summarized in Table 2. The ORFs, designated *dmpQ*, *E*, *F*, *G*, *H*, and *I*, have high G+C contents because of preferential usage of G and C at the third codon position, as has been found for the other genes of the pathway and for *Pseudomonas* genes in general (30, 48).

The *dmpQ* gene is located between *dmpP* and *dmpB*, whereas *dmpE*, *F*, *G*, *H*, and *I* are located downstream of *dmpD*. Thus, the coding order of the operon is *dmpKLM NOPQBCDEFGHI*, and the intergenic spacing varies between 0 and 70 nucleotides. At the *dmpQ-dmpB* and *dmpG-dmpH* junctions, the last base of the last codon of one gene is the first base of the ATG start of the next gene. The very tight clustering of the genes suggests that the 15 genes comprise a single operon. This is consistent with previous data where a transposon insert in *dmpP* inactivated the expression of downstream genes (40).

The nucleotide sequence was also analyzed for potential regulatory signals. A putative promoter region, 30 bp upstream from the transcriptional start of *dmpK*, was previously reported (30). This promoter region has strong homology to the *nif*-like promoters that have been shown to be regulated by the alternative σ^{54} factor (15, 25). No other regions with homology to either the *E. coli* −35 TTGACA −10 TATAAT or the *nif*-like −24 TGGC −12 TTGCT consensus sequences were found within the entire coding region. Likewise, no sequence similar to terminator regions (32) was found in the coding region or downstream of *dmpI*, the last gene of the operon. However, the nucleotide sequence downstream of *dmpI* has comparatively low G+C content, has A and T tracks, and shows no preferential codon usage in any of the three reading frames. Furthermore, the expression of this entire downstream region does not result in the production of detectable protein products (see below). These features suggest that this is noncoding DNA, but it remains to be determined how and where transcription terminates.

Polypeptide products of the *dmp* operon. The predicted and observed sizes of the polypeptide products of *dmpK*, *L*, *M*, *N*, *O*, *P*, *B*, *C*, and *D* were previously determined (Table 2). To investigate the size of the gene products of *dmpQ*, *E*, *F*, *G*, *H*, and *I*, a series of plasmids expressing different regions of the DNA spanning the operon were constructed by using the pMMB66EHΔ and pMMB66HEΔ *tac* expression vectors (Fig. 4A). To visualize polypeptide products, the plasmids were introduced into the maxicell strain CSR603, and the plasmid-encoded polypeptides were analyzed by SDS-PAGE (Fig. 4B).

Plasmid pVI300Δ contains DNA spanning *dmpQ* and part of *dmpB*. From the nucleotide sequence, this plasmid would be predicted to express two polypeptides, one of 12.2 kDa corresponding to the product of *dmpQ* and one of 25.0 kDa comprising the first 162 amino acid residues of the *dmpB* gene product fused to a sequence of 67 unrelated amino acid residues. pVI300Δ mediates production of two novel polypeptides, ΔB (23.0 kDa) and Q (12.0 kDa), of approximately the predicted molecular mass (Fig. 4B, lane 1). Plasmids pVI301Δ through pVI307Δ (Fig. 4B, lanes 4 through 10, respectively) contain overlapping regions of the operon and mediate production of different combinations of six novel polypeptides: D (30.0 kDa), E (28.0 kDa), F (35.0 kDa), G (39.0 kDa), H (28.5 kDa), and I (6.7 kDa). Polypeptide D (30.0 kDa) was previously shown to be the product of *dmpD* (3). Comparison of the DNA contents and polypeptides produced from each plasmid indicates that the polypeptides are encoded in the order D-E-F-(G or H)-(G or H)-I. Plasmids pVI308Δ through pVI314Δ (Fig. 4B, lanes 11 through 16, respectively) were used to map the relative order and location of the coding regions for the polypeptides more precisely. These plasmids express DNA spanning each of the genes *dmpD*, *E*, *F*, *G*, *H*, and *I* in turn. Each plasmid independently expresses a polypeptide indistinguishable on the basis of size from polypeptide D, E, F, G, H, or I. Some of these plasmids express the individual polypeptides at levels lower than those of plasmids expressing more than one gene; consequently, vector-encoded proteins can be seen more clearly in these lanes. The apparently decreased level of expression of the polypeptides from these plasmids might be the result of lower transcriptional levels because of promoter location and/or decreased translation due to mRNA stability or disruption of coupled transcription-translation that can occur on polycistronic mRNAs. Nevertheless, the results clearly demonstrate the relative coding order D-E-F-G-H-I and define the coding regions as follows: D, between *Hpa*I and *Sac*I (bp 8047 through 9070); E, between

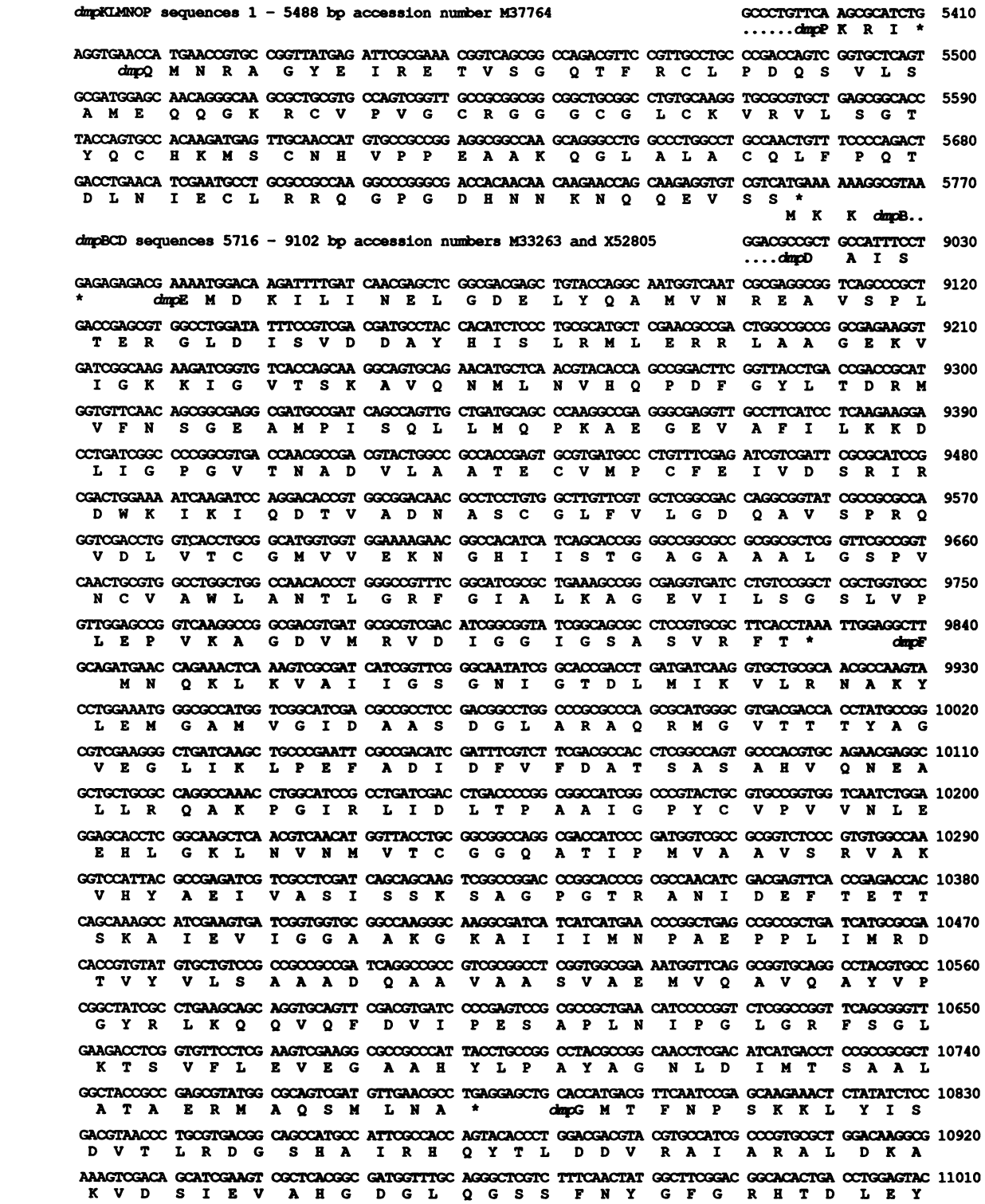

FIG. 3. Nucleotide sequence of the phenol/3,4-dmp catabolic operon. The sense strand is shown along with translation of six ORFs, designated *dmpQ* and *dmpEFGHI*, that are preceded by putative ribosome binding sites. The deduced amino acid sequences are shown in their one-letter code, and the asterisks indicate stop codons.

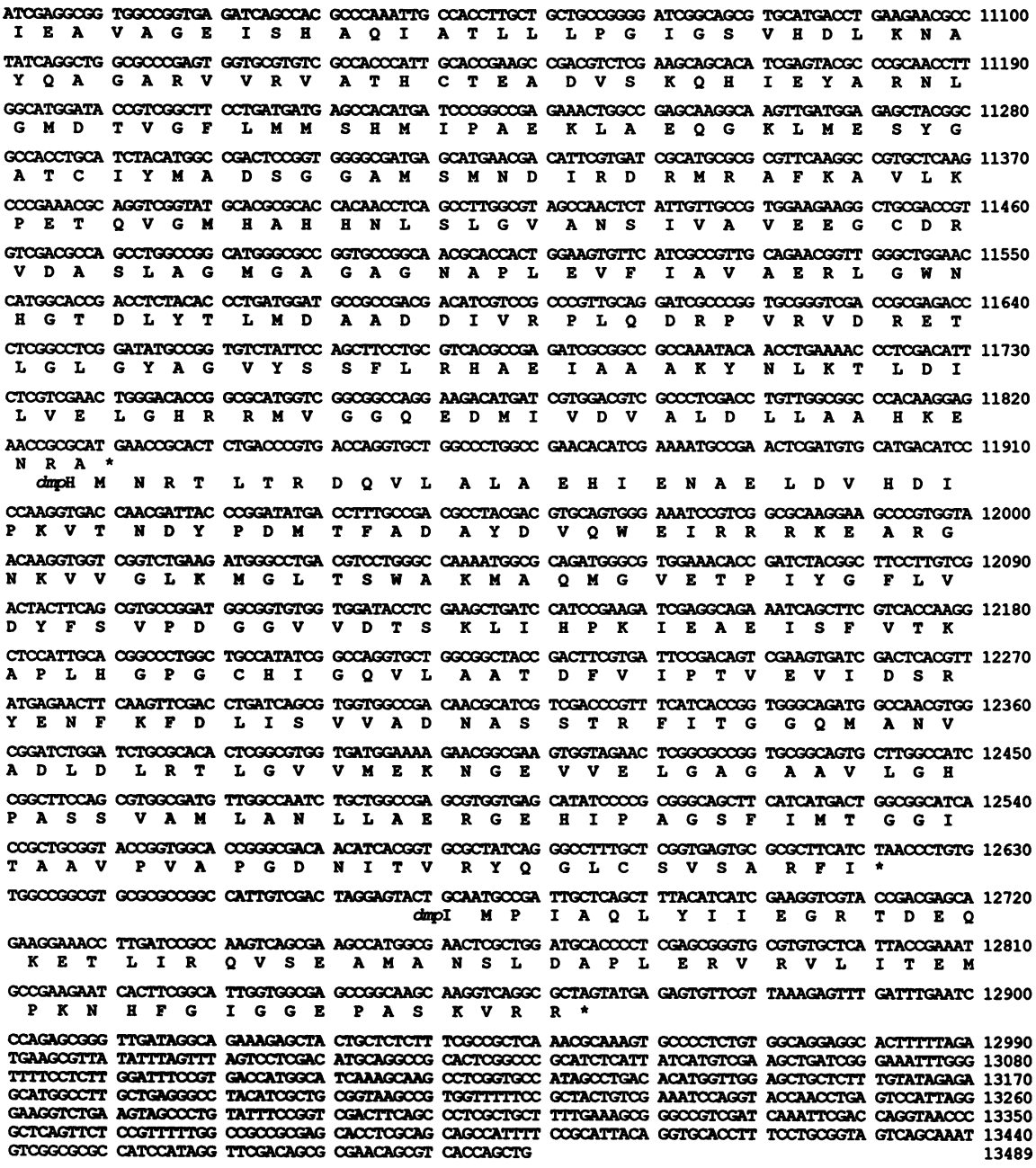

FIG. 3—*Continued.*

*Dde*I and *Eco*RI (bp 9033 through 10051); F, between *Sal*I and *Sal*I (bp 9790 through 10929); G, between *Sau*I and *Bst*EII (bp 10785 through 11921); H, between *Not*I and *Xho*I (bp 11702 through 12784); and I, between *Sca*I and *Pvu*II (bp 12670 through 13489). Hence, the sizes and order of polypeptides correlate well with the sizes and order of the genes (Table 2).

The plasmids pVI302Δ and pVI305Δ through pVI307Δ carry DNA in addition to coding regions. The additional DNA ranges from approximately 0.63 to 7.04 kb downstream from the end of *dmpI*. However, these plasmids do not mediate the production of any polypeptides other than those defined above (Fig. 4B, lanes 5, 8, 9, and 10). This observation suggests either that transcriptional termination occurs soon after the end of the *dmpI* coding region or that this is a noncoding region.

Lower *meta*-cleavage enzyme activities. The four known activities of the *meta*-cleavage pathway that have not previously been assigned to *dmp* gene products are 4-oxalocrotonate isomerase, 4-oxalocrotonate decarboxylase, 2-oxopent-4-enoate hydratase, and 4-hydroxy-2-oxovalerate aldolase. Crude extracts from cells harboring pVI265 and pVI299, which express the complete pathway from the IPTG-inducible *tac* promoter, contain approximately 25 to 50% of the levels of these enzymes found in crude extracts from phenol-grown wild-type strain CF600 (Table 3). Crude extracts from a vector-bearing control strain showed only basal levels of these enzyme activities, similar to those found for the

TABLE 2. Summary of the genes and gene products of the phenol/3,4-dmp catabolic operon

Gene	Coordinates (bp)	Intergenic spacing[a] (bp)	Putative ribosome binding sites[b]	% G+C in ORF	No. of amino acid residues	Molecular mass (kDa)		Function	Reference or source
						Predicted	Estimated		
dmpK	745–1020	55	CGCAAGCCGCCAACCTGGAGATG Met	59.4	92	10.6	12.5	Unknown	30, 33
dmpL	1076–2068	6	AACAAGAGGGTACGGTTGATATG Met	63.4	331	38.2	34.0	Phenol hydroxylase component	30, 33
dmpM	2075–2344	14	AAAGCCGCAAGGAATAAAGCATG Met	60.7	90	10.5	10.0	Phenol hydroxylase component	30, 33
dmpN	2359–3909	70	AAGAACTAGGAGACAAGCTCATG Met	59.4	517	60.5	58.0	Phenol hydroxylase component	30, 33
dmpO	3980–4336	13	AAGAACAAGAGGTTTCGATCATG Met	61.8	119	13.2	13.0	Phenol hydroxylase component	30, 33
dmpP	4350–5408	11	GTGCAGCTGAGAGGTGTGTCATG Met	65.6	353	38.5	39.0	Phenol hydroxylase component	30, 33
dmpQ	5420–5755	0	AAGCGCATCTGAGGTGAACCATG Met	64.5	112	12.2	12.0	Unknown	This study
dmpB	5755–6675	37	AACCAGCAAGAGGTGTCGTCATG Met	61.0	307	35.2	32.0	Catechol 2,3-dioxygenase	3, 4
dmpC	6713–8170	10	TTTTTGCAGAGATTGCGCAGATG Met	66.1	486	51.7	50.0	2-Hydroxymuconic semialdehyde dehydrogenase	3, 31
dmpD	8181–9029	14	CGTGAAGTTGTGAGGCAGCCATG Met	66.7	283	31.0	30.0	2-Hydroxymuconic semialdehyde hydrolase	3, 31
dmpE	9044–9826	18	ATTTCCTGAGAGAGACGAAAATG Met	64.2	261	27.9	28.0	2-Oxopent-4-dienoate hydratase	This study
dmpF	9845–10780	14	CCTAAATTGGAGGCTTGCAGATG Met	65.3	312	32.7	35.0	Acetaldehyde dehydrogenase (acylating)	This study
dmpG	10795–11829	0	AACGCCTGAGGAGCTGCACCATG Met	61.9	345	37.5	39.0	4-Hydroxy-2-oxovalerate aldolase	This study
dmpH	11829–12620	53	GCCCACAAGGAGAACCGCGCATG Met	59.9	264	28.4	28.5	4-Oxalocrotonate decarboxylase	This study
dmpI	12674–12862		TGTCGACTAGGAGTACTGCAATG Met	57.6	63	7.1	6.7	4-Oxalocrotonate isomerase	This study

[a] Numbers of base pairs between the indicated gene and the gene listed below it in column 1.
[b] Over- and underlined bases indicate sequences complementary to the 3' ends of the 16S rRNAs of *E. coli* and *P. aeruginosa*, respectively (39).

uninduced acetate-grown wild-type CF600 strain (Table 3). The background levels of 4-hydroxy-2-oxovalerate aldolase activities are relatively high. This is consistent with previous work, in which similar noninduced levels were observed in *E. coli* strains (8) and in certain *Pseudomonas* strains (37). Measurements of lower *meta*-cleavage pathway enzyme activities in *E. coli* strains expressing different combinations of *dmpE*, *F*, *G*, *H*, and *I* were used to correlate these genes with enzyme function.

***dmpI* encodes 4-oxalocrotonate isomerase activity.** The *dmpI* gene was found to encode 4-oxalocrotonate isomerase activity. Crude extracts from a strain harboring pVI314Δ, expressing *dmpI* alone, exhibited this activity (Table 3), albeit at a level significantly lower than that of extracts from strains expressing the whole operon. Crude extracts from a strain harboring pVI303Δ, which encodes *dmpDEFGH* but not *dmpI*, lack this activity (Table 3).

***dmpE* encodes 2-oxopent-4-enoate hydratase activity.** 2-Oxopent-4-enoate hydratase activity was found to be encoded by the *dmpE* gene, since crude extracts from a strain harboring pVI309Δ, expressing *dmpE* alone, contained this activity (Table 3). As observed for the isomerase, the hydratase activity when expressed in isolation was lower than that observed in crude extracts from strains expressing the complete pathway. Two possible explanations for this are lower expression levels and instability of the hydratase in the absence of another pathway enzyme(s). The specific activity of the hydratase from strains harboring pVI309Δ varied somewhat between experiments (twofold higher or lower than the activity shown in Table 3), suggesting the possibility of some instability of this enzyme. Strains harboring pVI303Δ (*dmpEFGH*) and pVI315Δ (*dmpEH*) contain reproducibly high hydratase activity levels. In the maxicell experiments (Fig. 4B, lanes 6 and 12), pVI303Δ and pVI309Δ express the *dmpE* gene product at similar levels; hence, the level of hydratase activity observed in the strain harboring pVI309Δ is somewhat lower than expected based on the apparent expression levels. Taken together, these data may indicate that the hydratase is less stable and/or less active in the absence of the *dmpH* product (see below). However, conclusive experiments must await purification of the enzymes.

***dmpH* encodes 4-oxalocrotonate decarboxylase activity.** One complication in determining which gene encodes 4-oxalocrotonate decarboxylase is the lack of 4-oxalocrotonate decarboxylase activity in the absence of the hydratase. The decarboxylases from the *meta*-cleavage pathways encoded by the TOL plasmid (20) and *P. putida* U (12) have been shown to be tightly associated with their respective hydratases; preliminary protein purification data from our laboratory suggest a similar tight association of the decarboxylase and hydratase from *Pseudomonas* sp. strain CF600 (unpublished observation). Attempts to express the TOL-encoded decarboxylase in isolation resulted in low or undetectable levels of activity (20), indicating the necessity for the presence of the hydratase for the detection of decarboxylase activity.

No 4-oxalocrotonate decarboxylase activity was detected

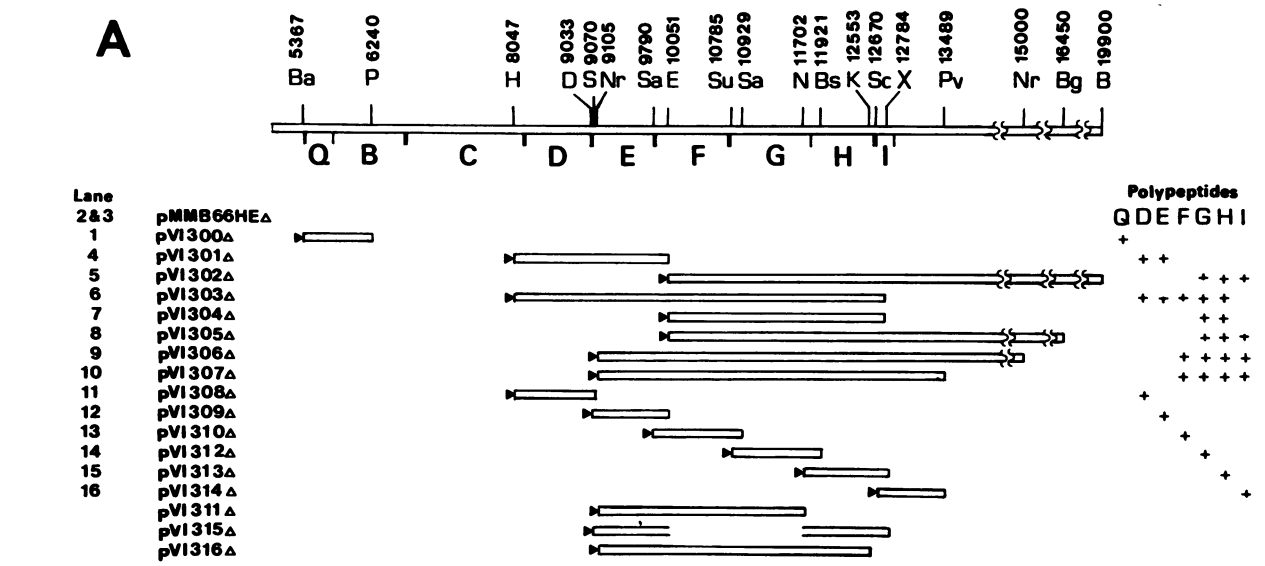

FIG. 4. Analysis of the polypeptides produced from the *dmpQ*, *D*, *E*, *F*, *G*, *H*, and *I* genes of the phenol/3,4-dmp operon. (A) The extent of the DNA in a plasmid series is shown with a summary of the polypeptides produced from the plasmids tested. Wavy lines indicate the locations of discontinuity in the scale. Coordinates of restriction endonuclease recognition sites are given in base pairs. B, *Bam*HI; Ba, *Bal* 31; D, *Dde*I; E, *Eco*RI; H, *Hpa*I; Nr, *Nru*I; Pv, *Pvu*II; S, *Sac*I; Sa, *Sal*I; Sc, *Sca*I; Su, *Sau*I. Only the sites used in the construction of plasmids are shown. (B) Maxicell analysis of plasmid-encoded polypeptides. Polypeptides from CSR603 harboring the plasmids indicated in panel A were separated by 15 to 20% acrylamide gradient SDS-PAGE with 32 mM NaCl in the analytical gel. Lanes 6 and 12 have half samples loaded to aid visualization of individual bands. The molecular mass standards are shown in kilodaltons. ΔB (23.0 kDa), Q (12.0 kDa), D (31.0 kDa), E (28.0 kDa), F (35.0 kDa), G (39.0 kDa), H (28.5 kDa), and I (6.7 kDa) indicate novel polypeptide bands encoded by the different plasmids. The relative molecular mass of polypeptide I was determined by using Pharmacia peptide standards (no. 17-055101; 17.21, 14.6, 8.24, 6.38, and 2.56 kDa) (data not shown).

from strains harboring plasmids expressing *dmpE*, *F*, *G*, *H*, or *I* in isolation (Table 3). However, decarboxylase activity was detected in all strains that coexpressed *dmpH* and *dmpE* (hydratase). Plasmid pVI315Δ expresses only *dmpE* and *dmpH*, and a strain harboring this plasmid has both hydratase (*dmpE*) and decarboxylase activities. Hence, *dmpH* is clearly associated with decarboxylase activity. No decarboxylase activity was detected from strains expressing *dmpH* in isolation (pVI313Δ), even when vastly increased amounts of crude extract protein were used in the assay. The polypeptide levels observed from plasmids pVI303Δ and pVI313Δ in maxicell experiments (Fig. 4B, lanes 6 and 15) indicate that pVI313Δ expresses the decarboxylase at an approximately fivefold lower level than does pVI303Δ. However, since strains harboring pVI303Δ exhibit decarboxylase activity that is approximately 100-fold higher than background levels, we would expect to be able to detect decarboxylase activity in strains harboring pVI313Δ, despite the fivefold lower expression level. Thus, we conclude that no decarboxylase activity was found in strains harboring pVI313Δ (*dmpH*) because of the absence of coexpression of the hydratase rather than because of low expression levels. Attempts to reconstitute decarboxylase activity by mixing extracts of strains expressing the *dmpE* and *dmpH* in isolation were unsuccessful (data not shown). This is consistent with the notion that these two gene products must be coexpressed to allow correct physical association.

***dmpG* encodes 4-hydroxy-2-oxovalerate aldolase activity.** In some bacteria that degrade aromatic compounds, 4-hydroxy-2-oxovalerate aldolase appears to be a noninducible enzyme (36). However, the results shown in Table 3 clearly demonstrate the inducible nature of this aldolase in *Pseudomonas* sp. strain CF600. The *dmpE*, *F*, and *I* genes encode specific *meta*-cleavage pathway activities (see above). Therefore, the 4-hydroxy-2-oxovalerate aldolase activity must be encoded by either *dmpF* or *dmpG*. As discussed below, *dmpF* alone encodes acetaldehyde dehydrogenase (acylating), leaving *dmpG* as the obvious candidate to encode the aldolase. Strains harboring either pVI303Δ (*dmpDEFGH*) or pVI316Δ (*dmpFG*) exhibit high aldolase activity at similar levels, whereas extracts from pVI311Δ (*dmpF*) contain no detectable aldolase activity. These results demonstrate the correlation between *dmpG* and the presence of aldolase activity. The expression of *dmpG* alone did not yield aldolase activity (pVI312Δ, Table 3). This result was surprising, on the basis of polypeptide levels expressed from pVI303Δ and pVI312Δ (Fig. 4B, lanes 6 and 14), which indicate a reduction of only 5- to 10-fold in polypeptide levels when *dmpG* is expressed on its own. Since pVI303Δ expresses aldolase activity at 15- to 20-fold above background, we would expect to detect aldolase activity in extracts from the pVI312Δ-bearing strain. Although we cannot completely rule out the possibility that low levels of expression from pVI312Δ may account for the lack of activity in this strain, an alternative explanation is possible. High aldolase activity in strains that coexpress *dmpF* and *dmpG* might indicate dependence of the aldolase activity on the presence of the

TABLE 3. Enzyme activities of strains expressing various genes of the phenol catabolic operon[a]

Extract	Enzyme activity				
	4OI (U/mg)	4OD (U/mg)	OEH (U/mg)	HOA (mU/mg)	ADA (mU/mg)
Pseudomonas sp. strain CF600 (wild type)					
Phenol grown	560	3.5	42	160	61[b] (140)
Acetate grown	<1	<0.02	0.2	7.6	− (−)
E. coli DH5					
pMMB66EHΔ (vector control)	<1	<0.02	<0.01	6.3	−
pVI265 (whole operon)	290	0.62	10	39	58
pVI299 (whole operon)	310	0.74	11	44	59
pVI303Δ (*dmpDEFGH*)	<1	2.0	18	120	79
pVI309Δ (*dmpE*)	<1	<0.02	3.3	8.4	−
pVI310Δ (*dmpF*)	<1	<0.02	<0.01	7.0	−
pVI311Δ (*dmpF*)	<1	<0.02	<0.01	6.4	90
pVI312Δ (*dmpG*)	<1	<0.02	<0.01	5.0	−
pVI313Δ (*dmpH*)	<1	<0.02	<0.01	6.1	−
pVI314Δ (*dmpI*)	61	<0.02	<0.01	6.5	−
pVI315Δ (*dmpEH*)	<1	1.9	28	7.9	−
pVI316Δ (*dmpFG*)	<1	<0.02	<0.01	104	62

[a] Enzyme assays were performed with crude extracts prepared as described in Materials and Methods. The figures represent the averages of duplicate determinations. Each experiment was performed a minimum of two times. −, not detectable. Enzyme abbreviations are as defined in the legend to Fig. 1.

[b] The reaction rate decreased very rapidly. The enzyme activity with a 10-fold-higher concentration of NAD^+ in the reaction mixture is given within parentheses.

dmpF gene product, acetaldehyde dehydrogenase (acylating). Experiments with a strain in which only *dmpF* has been deleted from the entire pathway suggest that this might be the case, since, in comparison with results from a strain expressing the complete pathway, both aldolase and acetaldehyde dehydrogenase (acylating) activities are undetectable, whereas all other lower pathway enzyme levels are essentially identical (unpublished data).

***dmpF* encodes acetaldehyde dehydrogenase (acylating) activity.** The fate of acetaldehyde (or propionaldehyde, in the case of 4-methyl-substituted catechols), which formed by the action of 4-hydroxy-2-oxovalerate aldolase, has not been rigorously determined. The presence of alcohol dehydrogenase activity in phenol-grown *P. putida* U was noted (12), and this represents one possible mechanism for metabolizing the aldehyde formed by the action of the aldolase. Alcohol dehydrogenase activity was also found, by using acetaldehyde or propionaldehyde as a substrate, in crude extracts from *Pseudomonas* sp. strain CF600 and was present at similar levels in extracts from cells grown at the expense of either phenol or acetate (data not shown). Although this noninducible enzyme may metabolize the aldehyde formed in the *meta*-pathway, an operon-encoded enzyme would provide a mechanism for greater control over the fate of this metabolite.

The *dmpF* gene encodes a previously undescribed operon-encoded enzyme activity of the *meta*-cleavage pathway. A strain harboring pVI311Δ, which encodes *dmpF* alone, expresses a coenzyme A-dependent acetaldehyde dehydrogenase (Table 3); no activity was observed in the absence of coenzyme A (data not shown). This activity was also found in two other strains that harbor plasmids expressing *dmpF* together with other genes of the pathway (pVI303Δ and pVI316Δ, Table 3). No enzyme activity was detected in extracts from a strain harboring pVI310Δ, which also encodes *dmpF*; however, the expression levels from this plasmid are very low (Fig. 4B, compare lanes 6 and 13). At low levels, this enzyme would be difficult to detect because of the presence of any competing alcohol dehydrogenase activity. This was a particular problem when measuring coenzyme A-dependent acetaldehyde dehydrogenase activity in extracts from *Pseudomonas* sp. strain CF600, which contained much higher levels of competing alcohol dehydrogenase activity compared with the low levels observed in *E. coli* strains (data not shown). Despite this problem, inducible coenzyme A-stimulated acetaldehyde dehydrogenase activity could be detected in phenol-grown but not acetate-grown wild-type CF600 cell extracts (Table 3). However, NADH production tapered off to zero almost immediately after the start of the reaction; although reaction time could be extended by using a 10-fold higher NAD^+ concentration, NADH production was still markedly nonlinear. Obviously, NADH produced by acetaldehyde dehydrogenase (acylating) can be consumed by the reduction of excess acetaldehyde by alcohol dehydrogenase present in the extract. Such an event would account for the quick tapering off of reactions observed for phenol-grown extracts.

DISCUSSION

The entire phenol/3,4-dmp catabolic pathway of *Pseudomonas* sp. strain CF600 is encoded in a single operon consisting of 15 genes, *dmpKLMNOPQBCDEFGHI*, with intergenic spacing that varies between 0 and 70 bp. The first six genes are involved in the conversion of phenol to catechol, and the remaining genes encode enzymes of the *meta*-cleavage pathway. This genetic organization is different than that found in two other phenol-degrading pseudomonads, *P. putida* U (5, 6) and *P. pickettii* PKO1 (26), in which the enzymes for conversion of phenol to catechol are encoded separately from their respective operons encoding the *meta*-cleavage pathway enzymes.

Computer-assisted data base searches with the six newly determined *meta*-cleavage enzyme sequences of *dmpQ*, *E*, *F*, *G*, *H*, and *I* did not reveal any striking homology to any genes of known function. However, the *dmpG* gene, which encodes 4-hydroxy-2-oxovalerate aldolase activity, showed approximately 20% identity over the entire length of the protein with the *nifV* gene product from various sources (1) and with α-isopropylmalate synthase from *Salmonella typhimurium* (35). The *nifV* gene appears to encode homocitrate synthase, which catalyzes aldol condensation of acetyl coenzyme A with α-ketoglutaric acid (22), whereas α-isopropylmalate synthase carries out condensation of acetyl coenzyme A and α- ketoisocitrate (44). Despite the differences in substrate structure and specificity, these condensation reactions are mechanistically simply the reverse of the 4-hydroxy-2-oxovalerate aldolase-catalyzed reaction. Thus, it is not surprising that these enzymes appear to be related.

The *dmpF* gene product encodes acetaldehyde dehydrogenase (acylating) activity. An enzyme (E.C.1.2.1.10) catalyzing this reaction was isolated from *Clostridium kluyveri* (10), but sequence information was not reported. The deduced amino acid sequence of the *dmpF* gene exhibited a short region of homology with a number of dehydrogenases. The region of homology (Fig. 5A) coincides with a βαβ fold fingerprint identified for ADP binding (47). The degree of agreement with the fingerprint (10 of 11 amino acid residues) and the requirement for the cofactor NAD^+ for enzymatic

FIG. 5. Primary amino acid sequence comparisons. Dashed lines indicate the locations and sizes of gaps inserted into the sequence. Identical amino acids are marked with colons, and chemically similar amino acids are marked with single dots. Amino acids considered to be similar are A, S, and T; D and E; N and Q; R and K; I, L, M, and V; and F, Y, and W. (A) Comparison of the N-terminal region of the deduced amino acid sequence of the *dmpF* gene product and a βαβ fold fingerprint region identified for ADP binding (45). Symbols: △, basic or hydrophobic (K, R, H, S, T, Q, N); □, small and hydrophobic (A, I, L, V, M, C); O, acidic (V, M). (B) Comparison of the deduced amino acid sequence of the *dmpQ* gene product and an analogously located ORF in the naphthalene *meta*-cleavage operon of NAH7 (47). Asterisks indicate cysteine residues with the same spacing as those found in [2Fe-2S] center-containing plant ferredoxins (43). Fifty-seven (52%) of 109 residues were found to be identical. (C) Comparison of the deduced amino acid sequences of the *dmpE* and *dmpH* gene products; 97 (37%) of 264 residues were found to be identical.

activity strongly suggest that this region participates in NAD^+ binding.

Acetaldehyde dehydrogenase (acylating) activity encoded by *dmpF* provides an operon-controlled mechanism for the metabolism of one of the products of the aldolase. The action of the aldolase results in the production of pyruvate, which can readily feed into the tricarboxylic acid cycle, and a short-chain aldehyde that requires further modification to produce a central metabolite. In the case of catechol or 3-methylcatechol, acetaldehyde would be produced, whereas propionaldehyde would be generated by the action of *meta*-cleavage enzymes on 4-methycatechol or 3,4-dimethylcatechol. Since the *dmpF*-encoded enzyme can use both of these aldehydes as substrates (unpublished data), it may be responsible for their further metabolism. Metabolism via this route would be energetically favorable, since it results in the production of NADH and the formation of an acyl coenzyme A ester that can readily be metabolized further.

A complicating factor in establishing the metabolic fate of acetaldehyde and propionaldehyde is the presence of noninducible, aldehyde-dependent NADH oxidation activity in crude extracts from *Pseudomonas* sp. strain CF600. It is most probable that this activity is due to alcohol dehydrogenase (E.C.1.1.1.1), which has also been shown to be present in crude extracts of phenol-degrading *P. putida* U (12). It is likely that this activity competes with the *dmpF*-encoded enzyme for any aldehyde that is formed, although to what extent it is important in the dissimilation of aldehydes is not clear. Due to the high NAD^+/NADH ratio generally present inside the cell (42), it is probable that reduction of acetaldehyde by alcohol dehydrogenase is thermodynamically unfavorable, whereas this ratio would favor the acetaldehyde dehydrogenase (acylating)-catalyzed reaction. However, additional information regarding the kinetic constants of the two enzymes is required to assess their relative importance. Despite the possible competition between these two aldehyde-metabolizing enzymes, the presence of alcohol dehydrogenase activity in itself does not necessarily indicate that another route for aldehyde dissimilation exists. In the absence of other alcohol-metabolizing enzymes, the reversible nature of the alcohol dehydrogenase-catalyzed reaction would mean that, as acyl coenzyme A is consumed, alcohol could be converted to the acyl coenzyme A derivative via the reaction catalyzed by the *dmpF*-encoded enzyme (10). In Results we also discuss the possibility that the coenzyme A-dependent dehydrogenase and the aldolase that produces the aldehyde are associated in some way. Such an association might represent a mechanism by which the aldehyde can be sequestered for metabolism via the *dmpF* gene product. Clearly, these reactions and the enzymes that catalyze them warrant more detailed studies.

Detailed study of the organization and function of a number of catabolic pathways has revealed that the order and nucleotide sequence of *meta*-pathway genes from different catabolic pathways can be highly conserved (2). This has led to the idea that the catabolic pathways may have evolved by inheritance of pre-evolved metabolic modules (11). Table 4 demonstrates the similarities between the sizes and organizations of the *meta*-cleavage pathway genes of the *dmp* operon of pVI150 and those of the *xyl* genes of TOL

TABLE 4. Comparison of the organizations of the *dmp* and *xyl meta* cleavage pathway genes[a]

Gene	Molecular mass of protein (kDa)	Enzyme encoded	Gene	Molecular mass of protein (kDa)	Enzyme encoded
dmpQ	12.0	Unknown	*xylT*	12.0	Unknown
dmpB	32.0	C23O	*xylE*	36.0	C23O
dmpC	50.0	2HMSD	*xylG*	60.0	2HMSD
dmpD	30.0	2HMSH	*xylF*	34.0	2HMSH
dmpE	28.0	OEH	*xylJ*	28.0	OEH
dmpF	35.0	ADA	*xylQ*	42.0	Unknown
dmpG	39.0	HOA	*xylK*	39.0	HOA
dmpH	28.5	4OD	*xylI*	27.0	4OD
dmpI	6.7	4OI	*xylH*	4.0	4OI

[a] Molecular mass estimates and correlations of polypeptides to enzyme functions are from reference 19; enzyme abbreviations are as defined in the legend to Fig. 1.

plasmid pWWO. The gene order of the naphthalene *meta*-cleavage pathway of NAH7 is the same except that the relative order of last two genes (encoding 4OD and 4OI) is reversed (21, 46). The order of the *xyl* and *dmp* genes is identical, and the gene product sizes, as determined by relative mobility on gels, are similar (Table 4). The largest difference in gene product size is observed between *dmpF*, which encodes an acetaldehyde dehydrogenase (acylating), and *xylQ*, an analogously located gene of unknown function within the *xyl* operon. Given the similarity of function of all the other *meta*-cleavage pathway genes, it would appear likely, despite the apparent difference in size, that *xylQ* encodes an isofunctional enzyme. The products of *dmpI* and *xylH*, which both encode 4OI, also appear to be different in size. However, we believe that this may be primarily a reflection of the PAGE systems and standards used to determine the apparent molecular mass, since the *dmpI* product appears as a 3.5-kDa band on tricine gels, but as a 6.7-kDa band on 20% or 10 to 20% or 15 to 20% gradient SDS-PAGE gels (data not shown).

The function of *dmpQ* is unknown, but coding regions of the same size and location are present in the *meta*-cleavage pathway operons of pWWO and NAH7 (Table 4) (19, 47). Comparison of the deduced amino acid sequences of *dmpQ* and the analogously located gene of NAH7 reveals 52% identity. The *dmpQ* gene product, like that of NAH7, has homology to ferredoxins and contains cysteine residues with the same spacing as the [2Fe-2S] center ligands in plant-type ferredoxins (Fig. 5B). These features suggest a possible role for the *dmpQ* product as an electron carrier for some step in the catabolism of phenol and/or its methyl-substituted derivatives.

Sequence identity between the genes encoding C230 of the three operons, *dmpB*, *xylE*, and *nahH* is between 83 and 87% on the amino acid level (4). This figure is significantly higher than that found for *dmpQ*. The results of data base searches with the sequences of *dmpC* and *dmpD* have been discussed (31). Although nucleotide sequence data for the isofunctional genes from the *xyl* and *nah* operons are not available in the data bases, our recent searches for homology to the *dmpD* gene product (2-hydroxymuconic semialdehyde hydrolase) identified partial ORFs upstream from the coding regions for the toluene dioxygenase genes of *P. putida* F1 (48) and benzene dioxygenase genes of *P. putida* (24). The degrees of identity found between the C-terminal portion of 2-hydroxymuconic semialdehyde hydrolase and the deduced amino acid sequence of the 3′ partial ORFs were 65.1 and 62.4% in a 175- and 101-amino acid overlap, respectively. Thus, although the catabolic pathways of pVI150, pWWO, and NAH7 may have inherited their *meta*-cleavage genes as an ancestral metabolic module, in other cases, such as toluene catabolic pathway of *P. putida* F1 and the benzene catabolic pathway, this apparently has not occurred or the genes have subsequently been reshuffled. Alternatively, and more likely in view of the conserved sequence and gene order between these two catabolic pathways (48), they may represent divergence from an alternative metabolic module.

The gene organization of the *meta*-cleavage pathway of *Pseudomonas pickettii* PKO1, which can grow at the expense of toluene, benzene, cresols, and phenol, was recently described (26). The organization of the *meta*-cleavage pathway genes differs from that described above for TOL and pVI150; the relative order of the genes encoding 2-hydroxymuconic semialdehyde dehydrogenase and 2-hydroxymuconic semialdehyde hydrolase is reversed, and the gene encoding 2-oxopent-4-enoate hydratase is located at the end of the operon. Some enzymes of this *meta*-cleavage pathway also appear to differ from those of TOL and pVI150 in that

TABLE 5. Homology within the *dmp* operon: comparison of primary amino acid sequences

Gene	% Identity[a] with:														
	dmpK	*dmpL*	*dmpM*	*dmpN*	*dmpO*	*dmpP*	*dmpQ*	*dmpB*	*dmpC*	*dmpD*	*dmpE*	*dmpF*	*dmpG*	*dmpH*	*dmpI*
dmpK	100.0	7.6	10.0	8.7	12.0	10.9	4.3	5.4	7.6	5.4	5.4	7.6	14.1	7.6	11.1
dmpL		100.0	10.0	5.4	8.4	7.6	7.1	7.8	5.4	6.7	5.7	7.1	7.6	8.0	9.5
dmpM			100.0	8.9	6.7	12.2	8.9	8.9	7.8	7.8	13.3	8.9	7.8	10.0	12.7
dmpN				100.0	8.4	5.7	8.0	6.2	6.8	4.9	6.1	7.1	7.2	7.2	7.9
dmpO					100.0	7.6	8.9	5.9	5.0	9.2	8.4	8.4	6.7	6.7	6.4
dmpP						100.0	11.6	6.5	9.1	8.1	6.5	7.4	10.4	6.4	11.1
dmpQ							100.0	5.4	8.0	9.8	7.1	10.7	8.0	5.4	12.7
dmpB								100.0	5.9	6.0	7.7	5.5	7.2	8.0	7.9
dmpC									100.0	6.7	11.1	9.9	6.1	6.8	14.3
dmpD										100.0	8.0	9.2	10.6	9.1	9.5
dmpE											100.0	8.4	7.3	30.3	11.1
dmpF												100.0	7.4	8.0	12.7
dmpG													100.0	9.1	6.4
dmpH														100.0	11.1
dmpI															100.0

[a] Percent identity found by using the PC-GENE software program Palign with gap and unit gap costs of 100.

4-oxalocrotonate decarboxylase can apparently function in the absence of 2-oxopent-4-enoate hydratase (see below). These results suggest earlier divergence of this catabolic pathway.

Gene duplication and subsequent divergence make up one mechanism by which different enzymatic activities might evolve. To investigate whether such a mechanism played a role in the formation of the *dmp* catabolic operon, the amino acid sequences of each of the 15 gene products of the pathway were compared. The PC-Gene software program Palign and the Wisconsin Genetics Computer Group software program Bestfit gave similar qualitative results. The results with the Palign program are shown in Table 5.

From the results shown in Table 5, the only obvious case in which ancestral gene duplication may have resulted in divergence to two different enzymatic activities involves the products of *dmpE* and *dmpH*, which encode 2-oxopent-4-enoate hydratase and 4-oxalocrotonate decarboxylase, respectively. These two proteins, when optimally aligned, show 37% identity; the greatest homology is in the C-terminal portions of the sequences (Fig. 5C). As described in Results, a strain harboring a plasmid expressing *dmpE* alone exhibited 2-oxopent-4-enoate hydratase activity, whereas expression of *dmpH* in isolation did not yield 4-oxalocrotonate decarboxylase activity. 4-Oxalocrotonate decarboxylase activity was only detected when *dmpE* and *dmpH* were coexpressed in the same cell and could not be restored by mixing crude extracts from strains expressing each of the genes in isolation. These data are consistent with the findings of Haryama et al. (20). They found that the two isofunctional enzymes from the toluene catabolic pathway copurify through three chromatography steps and probably form a complex within the cell. Similarly, these workers also found that expression of the two proteins separately results in active 2-oxopent-4-enoate hydratase but loss of 4-oxalocrotonate decarboxylase activity. Their data are consistent with a tetrameric association of the two proteins in a complex. It is possible that homomultimers or monomers of 2-oxopent-4-enoate hydratase retain activity, whereas heteromultimers of 2-oxopent-4-enoate hydratase and 4-oxalocrotonate decarboxylase are required for 4-oxalocrotonate decarboxylase activity.

Harayama et al. (20) postulate that the physical association of 2-oxopent-4-enoate hydratase and 4-oxalocrotonate decarboxylase might ensure efficient transformation of the unstable 2-oxopent-4-enoate hydratase substrate (Fig. 1, compound VI). They also point out that this intermediate can be produced and efficiently metabolized by the hydrolytic branch of the *meta*-cleavage pathway (Fig. 1, step 3) in the absence of any apparent physical association of the enzymes involved. The common ancestry and structural similarity of 2-oxopent-4-enoate hydratase and 4-oxalocrotonate decarboxylase might explain why a mechanism involving physical association of enzymes evolved for only the 4-oxalocrotonate branch of the pathway.

ACKNOWLEDGMENTS

We thank P. A. Williams for the kind gift of 4-oxalocrotonate, R. H. Olsen and J. J. Kukor for providing *P. putida* U, and M. Gullberg for critical reading of the manuscript and invaluable technical assistance.

This work was supported by the Swedish Natural Science Research Council (V.S. and J.P.), the Swedish Research Council for Engineering Sciences, the Center for Environmental Research (V.S.), the Natural Sciences and Engineering Research Council of Canada, and Concordia University (J.P.).

ADDENDUM

During the processing of the manuscript, nucleotide sequences of four *xyl* genes of the TOL-encoded *meta*-cleavage pathway were published: *xylT*, which is analogous to *dmpQ* (18a), and *xylGFJ*, which is analogous to *dmpCDE* (22a). Furthermore, the ORF upstream of the toluene dioxygenase genes of *P. putida* F1, *todF*, was characterized (28a), and the deduced amino acid sequence was aligned with that of *dmpD*.

REFERENCES

1. **Arnold, W., A. Rump, W. Klipp, U. B. Priefer, and A. Puehler.** 1988. Nucleotide sequence of a 24,206-base-pair DNA fragment carrying the entire nitrogen fixation gene cluster of *Klebsiella pneumoniae*. J. Mol. Biol. **203**:715–738.
2. **Assinder, S. J., and P. A. Williams.** 1990. The TOL plasmids: determinants of the catabolism of toluene and xylenes. Adv. Microb. Physiol. **31**:1–69.
3. **Bartilson, M., I. Nordlund, and V. Shingler.** 1990. Location and gene organization of the dimethylphenol catabolic genes of *Pseudomonas* CF600. Mol. Gen. Genet. **220**:294–300.
4. **Bartilson, M., and V. Shingler.** 1989. Nucleotide sequence and expression of the catechol 2,3-dioxygenase-encoding gene of phenol catabolizing *Pseudomonas* CF600. Gene **85**:233–238.
5. **Bayly, R. C., and M. G. Barbour.** 1984. The degradation of aromatic compounds by the *meta* and gentisate pathways, p. 253–294. *In* D. T. Gibson (ed.), Microbial degradation of organic compounds. Marcel Dekker, Inc., New York.
6. **Bayly, R. C., G. J. Wigmore, and D. L. McKenzie.** 1977. Regulation of the enzymes of the *meta*-cleavage pathway of *Pseudomonas putida*: the regulon is composed of two operons. J. Gen. Microbiol. **100**:71–79.
7. **Brown, R. E., K. L. Jarvis, and K. J. Hyland.** 1989. Protein measurement using bicinchoninic acid: elimination of interfering substances. Anal. Biochem. **180**:136–139.
8. **Burlingame, R., and P. J. Chapman.** 1983. Catabolism of phenylpropionic acid and its 3-hydroxy derivative by *Escherichia coli*. J. Bacteriol. **155**:113–121.
9. **Burlingame, R., and P. J. Chapman.** 1983. Stereospecificity in *meta*-fission catabolic pathways. J. Bacteriol. **155**:424–426.
10. **Burton, R. M., and E. R. Stadtman.** 1953. The oxidation of acetaldehyde to acetyl coenzyme A. J. Biol. Chem. **202**:873–890.
11. **Cane, P. A., and P. A. Williams.** 1986. A restriction map of naphthalene catabolic plasmid pWW60-1 and location of some of its catabolic genes. J. Gen. Microbiol. **132**:2919–2929.
12. **Collinsworth, W. L., P. J. Chapman, and S. Dagley.** 1973. Stereospecific enzymes in the degradation of aromatic compounds by *Pseudomonas putida*. J. Bacteriol. **113**:922–931.
13. **Dagley, S.** 1986. Biochemistry of aromatic hydrocarbon degradation in pseudomonads, p. 527–556. *In* J. R. Sokatch (ed.), The bacteria, vol. 10. The biology of *Pseudomonas*. Academic Press, Inc. (London), Ltd., London.
14. **Dagley, S., and D. T. Gibson.** 1965. The bacterial degradation of catechol. Biochem. J. **95**:466–474.
15. **Dixon, R.** 1986. The *xyl*ABC promoter from *Pseudomonas putida* TOL plasmid is activated by nitrogen fixation regulatory genes in *Escherichia coli*. Mol. Gen. Genet. **203**:129–136.
16. **Fürste, J. P., W. Pansegrau, R. Frank, H. Blöcker, P. Scholz, M. Bagdasarian, and E. Lanka.** 1986. Molecular cloning of the RP4 DNA primase region in a multirange *tac*P expression vector. Gene **48**:119–131.
17. **Hanahan, D.** 1985. Techniques for transformation of *E. coli*, p. 109–136. *In* D. M. Glover (ed.), DNA cloning, vol. 1. A practical approach. IRL Press Ltd., Oxford.
18. **Harayama, S., P. R. Lehrbach, and K. N. Timmis.** 1984. Transposon mutagenesis analysis of *meta*-cleavage operon genes of the TOL plasmid of *Pseudomonas putida* mt-2. J. Bacteriol. **160**:251–255.

18a. **Harayama, S., A. Polissi, and M. Rekik.** 1991. Divergent evolution of chloroplast-type ferredoxins. FEBS Lett. **285**:85–88.

19. **Harayama, S., and M. Rekik.** 1990. The *meta* cleavage operon of TOL degradative plasmid pWWO comprises 13 genes. Mol. Gen. Genet. **221**:113–120.
20. **Harayama, S., M. Rekik, K.-L. Ngai, and L. N. Ornston.** 1989. Physically associated enzymes produce and metabolize 2-hydroxy-2,4-dienoate, a chemically unstable intermediate formed in catechol metabolism via *meta* cleavage in *Pseudomonas putida*. J. Bacteriol. **171**:6251–6258.
21. **Harayama, S., M. Rekik, A. Wasserfallen, and A. Bairoch.** 1987. Evolutionary relationships between catabolic pathways for aromatics: conservation of gene order and nucleotide sequences of catechol oxidation genes of pWWO and NAH7 plasmids. Mol. Gen. Genet. **210**:241–247.
22. **Hoover, T. R., A. D. Robertson, R. L. Cerny, R. N. Hayes, J. Imperial, V. K. Shah, and P. W. Ludden.** 1987. Identification of the V factor needed for synthesis of the iron-molybdenum cofactor of nitrogenase as homocitrate. Nature (London) **329**: 855–857.
22a. **Horn, J. M., S. Harayama, and K. N. Timmis.** 1991. DNA sequence determination of the TOL plasmid (pWW0) *xyl* GIJ genes of *Pseudomonas putida*: implications for the evolution of aromatic catabolism. Mol. Microbiol. **5**:2459–2474.
23. **Hughes, E. J. L., and R. C. Bayly.** 1983. Control of catechol *meta*-cleavage pathway in *Alcaligenes eutrophus*. J. Bacteriol. **154**:1363–1370.
24. **Irie, S., S. Doi, T. Yorifuji, M. Takagi, and K. Yano.** 1987. Nucleotide sequence and characterization of the genes encoding benzene oxidation enzymes of *Pseudomonas putida*. J. Bacteriol. **169**:5174–5179.
25. **Köhler, T., S. Harayarma, J.-L. Ramos, and K. T. Timmis.** 1989. Involvement of *Pseudomonas putida* RpoN σ factor in regulation of various metabolic functions. J. Bacteriol. **171**: 4326–4333.
26. **Kukor, J. J., and R. H. Olsen.** 1991. Genetic organization and regulation of a *meta* cleavage pathway for catechols produced from catabolism of toluene, benzene, phenol, and cresols by *Pseudomonas pickettii* PKO1. J. Bacteriol. **173**:4587–4594.
27. **Kushner, S. R.** 1978. An improved method for transformation of *Escherichia coli* with ColE1 derived plasmids, p. 17–23. *In* H. W. Boyer and S. Nicosia (ed.), Genetic engineering. Elsevier/North Holland Publishing Co., Amsterdam.
28. **Laemmli, U. K.** 1970. Cleavage of structural proteins during the assembly of the head of the bacteriophage T4. Nature (London) **227**:680–685.
28a. **Menn, F.-M., G. J. Zylstra, and D. T. Gibson.** 1991. Location and sequence of the *tadF* gene encoding 2-hydroxy-6-oxohepta-2,4-dienoate hydrolase in *Pseudomonas putida* F1. Gene **104**: 91–94.
29. **Nishizuka, Y., A. Ichiyama, S. Nakamura, and O. Hayaishi.** 1962. A new metabolic pathway of catechol. J. Biol. Chem. **237**:PC268–PC270.
30. **Nordlund, I., J. Powlowski, and V. Shingler.** 1990. Complete nucleotide sequences and polypeptide analysis of multicomponent phenol hydroxylase from *Pseudomonas* sp. strain CF600. J. Bacteriol. **172**:6826–6833.
31. **Nordlund, I., and V. Shingler.** 1990. Nucleotide sequences of the *meta*-cleavage pathway enzymes 2-hydroxymuconic semialdehyde dehydrogenase and 2-hydroxymuconic semialdehyde hydrolase from *Pseudomonas* CF600. Biochim. Biophys. Acta **1049**:227–230.
32. **Platt, T.** 1986. Transcription termination and the regulation of gene expression. Annu. Rev. Biochem. **55**:339–372.
33. **Powlowski, J., and V. Shingler.** 1990. In vitro analysis of polypeptide requirements of multicomponent phenol hydroxylase from *Pseudomonas* sp. strain CF600. J. Bacteriol. **172**: 6834–6940.
34. **Reineke, W., and H.-J. Knackmuss.** 1988. Microbial degradation of haloaromatics. Annu. Rev. Microbiol. **42**:263–287.
35. **Ricca, E., and J. M. Calvo.** 1990. The nucleotide sequence of *leu*A from *Salmonella typhimurium*. Nucleic Acids Res. **18**: 1290.
36. **Sala-Trepat, J. M., and W. C. Evans.** 1971. The *meta* cleavage of catechol by *Azotobacter* species: 4-oxalocrotonate pathway. Eur. J. Biochem. **20**:400–413.
37. **Sala-Trapat, J. M., K. Murray, and P. A. Williams.** 1972. The metabolic divergence in the *meta* cleavage of catechols by *Pseudomonas putida* NCIB 10015: physiological significance and evolutionary implications. Eur. J. Biochem. **28**:347–356.
38. **Sancar, A., A. M. Hack, and W. D. Rupp.** 1978. Simple method for the identification of plasmid-coded proteins. J. Bacteriol. **137**:692–693.
39. **Shine, J., and L. Dalgarno.** 1975. Determination of cistron specificity in bacterial ribosomes. Nature (London) **254**:34–38.
40. **Shingler, V., M. Bagdarsarian, D. Holroyd, and F. C. H. Franklin.** 1989. Molecular analysis of the plasmid encoded phenol hydroxylase of *Pseudomonas* CF600. J. Gen. Microbiol. **135**:1083–1092.
41. **Simon, R., U. Priefer, and A. Pühler.** 1983. A broad host range mobilization system for *in vivo* genetic engineering: transposon mutagenesis in Gram-negative bacteria. Biotechnology **1**:784–790.
42. **Stanier, R. Y., J. L. Ingraham, M. L. Wheelis, and P. R. Painter.** 1987. General Microbiology, p. 81. MacMillan Education Ltd., London.
43. **Stout, C. D.** 1982. Iron-sulfur protein crystallography, p. 97–146. *In* T. G. Spiro (ed.), Iron sulfur proteins. John Wiley & Sons, Inc., New York.
44. **Strassman, M., and L. N. Ceci.** 1963. Enzymatic formation of α-isopropylmalic acid, an intermediate in leucine biosynthesis. J. Biol. Chem. **238**:2445–2452.
45. **Wierenga, R. K., P. Terpstra, and W. G. J. Hol.** 1986. Prediction of the occurrence of the ADP-binding β-α-β fold in proteins using an amino acid sequence fingerprint. J. Mol. Biol. **187**:101–107.
46. **Yen, K. M., and I. C. Gunsalus.** 1982. Plasmid gene organization: naphthalene/salicylate oxidation. Proc. Natl. Acad. Sci. USA **79**:874–878.
47. **You, I.-S., D. Ghosal, and I. C. Gunsalus.** 1991. Nucleotide sequence analysis of the *Pseudomonas putida* PpG7 salicylate hydroxylase gene (*nahH*) and its 3′ flanking region. Biochemistry **30**:1635–1641.
48. **Zylstra, G. J., and D. T. Gibson.** 1989. Toluene degradation by *Pseudomonas putida* F1: nucleotide sequence of the *todC1 C2BADE* genes and their expression in *E. coli*. J. Biol. Chem. **264**:14940–14946.